Orbital Damping of the Oscillating Superfluid ^{3}He A–B Interface at Low Temperatures

**M. Arrayás · S. N. Fisher · R. P. Haley ·
G. R. Pickett · M. Skyba**

Abstract We present a model for the friction and effective mass of an oscillating superfluid ^{3}He A–B interface due to orbital viscosity in the B-phase texture close to the interface. The model is applied to an experiment in which the A–B interface was stabilised in a magnetic field gradient at the transition field $B_c = 340$ mT at 0 bar pressure and at a very low temperature $T \approx 0.155$ mK. The interface was then oscillated by applying a small additional field at frequencies in the range 0.1–100 Hz. The response of the interface is governed by friction and by its effective mass. The measured dissipation does not fit theoretical predictions based either on the Andreev scattering of thermal quasiparticles or by pair-breaking from the moving interface. We describe a new mechanism based on the redistribution of thermal quasiparticle excitations in the B-phase texture engendered by the moving interface. This gives rise to friction via orbital viscosity and generates a significant effective mass of the interface. We have incorporated this mechanism into a simple preliminary model which provides reasonable agreement with the measured behaviour.

1 Introduction

The A–B interface is the most ordered interface available for experimental study [1]. The two bulk phases have different symmetries, with well-understood and established

S. N. Fisher · R. P. Haley (✉) · G. R. Pickett · M. Skyba
Department of Physics, Lancaster University, Lancaster, UK
e-mail: r.haley@lancaster.ac.uk

M. Arrayás
Área de Electromagnetismo, Universidad Rey Juan Carlos, Camino del Molino s/n, 28943 Fuenlabrada, Madrid, Spain

order parameters. When an interface between the A and B phases is stabilised, the order parameter varies smoothly between the two, passing through a planar-like state [2–5]. In thermodynamic terms the phase transition between the A and B phases is first order with a corresponding latent heat [6,7], and the interface has an associated surface tension [8–12].

The analogies between the order parameters of superfluid ^{3}He and those describing other fundamental systems allow us to use the superfluid as an exemplar for the experimental investigation of a broad range of phenomena [13]. For instance the structure of the order parameters which develop as the fluid passes through symmetry-breaking phase transitions are similar to the broken symmetries of the metric of the Universe. The superfluid thus provides a test-bed for the study of transitions in the quantum vacuum state of the early Universe [14,15], and the A–B interface can simulate a 2-brane [16].

Here we focus on the dynamical behaviour of the A–B interface. Previous experiments by Buchanan et al. [17] on a fast freely-moving interface in low magnetic fields found values for the friction that were in line with theoretical estimates based on the Andreev scattering of thermal quasiparticle excitations [18]. Later measurements were made in Lancaster on a controlled oscillating interface in high magnetic fields and at much lower temperatures [19]. In this case the friction was found to be orders of magnitude higher than theoretical predictions [1,18,20]. Furthermore, the friction was found to have an unexpected frequency dependence [19].

Below, we show that the behaviour of an oscillating A–B interface in high magnetic fields and low temperatures is dominated by orbital viscosity [21] and by a significant effective mass generated by thermal quasiparticle excitations in the B-phase order parameter texture.

In zero magnetic field the B phase is pseudo-isotropic, with no net spin or orbital angular momentum, and an isotropic energy gap Δ_0 [22]. In a magnetic field the B-phase order parameter is distorted and the energy gap is suppressed along the orbital anisotropy axis l_B, producing intrinsic spin and orbital angular momentum [21]. Further, in the large magnetic fields needed to stabilise the A phase the B-phase anisotropy is dominated by significant Zeeman splitting. Thus a large density of thermal excitations occupy states along the l_B axis. The orientation of l_B is influenced by the presence of the A–B interface [5] so as the interface moves the orientation changes and the thermal excitations must redistribute. This generates substantial dissipation related to orbital viscosity. The redistribution also has a significant reactive component which can be characterised as an effective mass of the interface.

2 The Experiment

The experiments were performed on a sample of superfluid ^{3}He contained in a sapphire tube connected to the inner cell of a Lancaster-style nuclear cooling stage, shown in Fig. 1 and described earlier in more detail [7]. The sapphire tube has internal diameter 4.3 mm and length 44 mm, sealed at the bottom and closed at the top by a thin
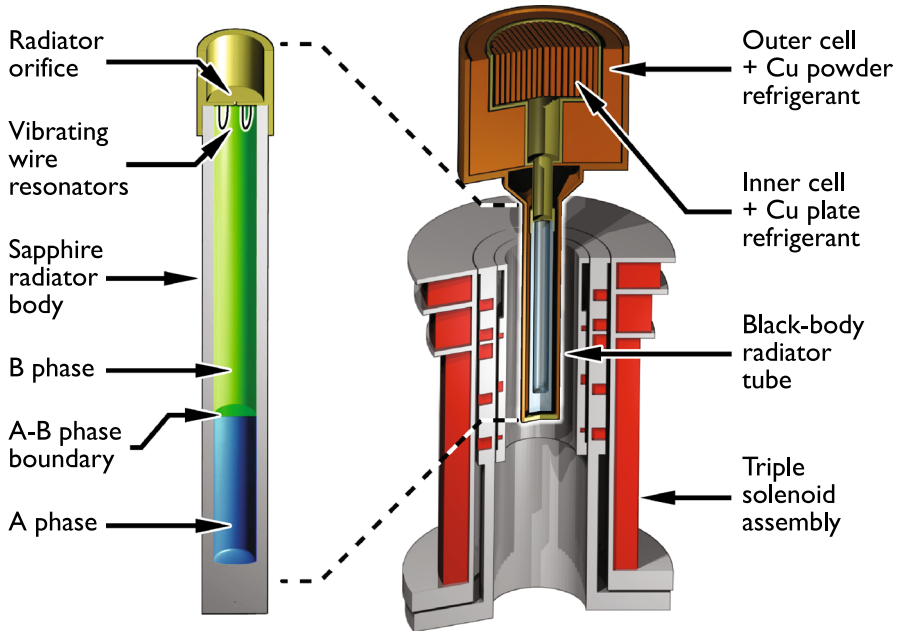
Fig. 1 The experimental cell showing the sapphire black body radiator that contains the A–B interface, and the multiple solenoid stack used for creating and manipulating the field profiles (Colour figure online)

sheet of stycast-impregnated paper with a small 0.5 mm diameter orifice connecting it to the inner cell. This small hole provides a weak thermal link to the thermal bath and the sapphire tube can be treated as a pseudo black body radiator for quasiparticle excitations [6,23]. The temperature of the sample was monitored by measuring the quasiparticle density inferred from the damping of a 4.5 μm diameter NbTi vibrating wire resonator (VWR) [24]. A 13 μm NbTi VWR was used as a heater. The VWRs were at the top of the cell where the magnetic field was always relatively small, on the order of 50 mT. At these low fields the energy gap of the B phase is approximately isotropic and the damping width Δf_2 of the VWR resonance is proportional to $\exp(-\Delta_0/k_B T)$, allowing for reliable thermometry [25].

The experiments were carried out at 0 bar pressure with a base temperature of 146 μK, determined by an equilibrium between the heat leak into the sapphire tube and the power carried by quasiparticles leaving through the orifice. We calibrated the change in Δf_2 of the thermometer VWR as a function of power by dissipating known amounts of heat in the tube using the heater VWR [23,25]. This enabled us to then use the thermometer VWR to measure power dissipation owing to motion of an A–B interface in the lower section of the tube.

A solenoid stack was used to create a shaped magnetic field profile to stabilise the A phase in the bottom of the tube in fields above the transition field $B_c = 340$ mT [6, 7,26], whilst maintaining the top of the tube with the VWRs in low field B phase. Once the A–B interface was established across the tube, a small additional alternating field was applied to oscillate the interface over a range of frequencies.

3 Modelling the Interface Dynamics

Referring to Fig. 2, in equilibrium the A–B interface is located at a vertical position z_{eq} where the magnetic field is equal to the transition field B_c. The magnetic field is approximately uniform in the horizontal plane so we can assume that the interface is flat. We ignore the small effect of surface tension [12] and wetting at the cell walls [9] since they give rise to a meniscus on the order of 0.1 mm, much smaller than the diameter of the sapphire tube. When the field profile is adjusted, the position of B_c changes, and the interface experiences a restoring force towards the new equilibrium position. The magnitude of the restoring force per unit area is equal to the difference in Gibbs free energy per unit volume $\Delta G_{AB}(B)$ between the two phases at the interface which is in a field B.

The field dependence of the Gibbs free energy for a material of magnetic susceptibility χ is given by

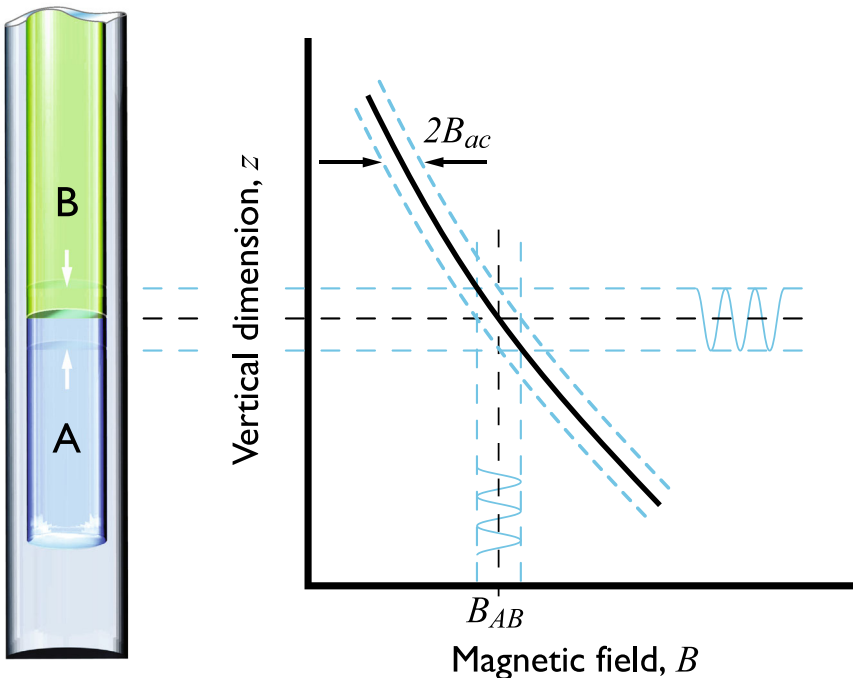$$G(B) = G(0) - \frac{1}{2}\chi B^2 \qquad (1)$$

Fig. 2 The *bottom end* of the sapphire black body radiator contains A phase in the *bottom* and B phase in the *top*. The A–B interface is stabilised at a position z_{eq} corresponding to the transition field B_c by a shaped magnetic field profile (*solid line*) provided by the solenoid stack. Oscillating the field profile oscillates the equilibrium position z_{eq} along the cell axis. The oscillatory response of the A–B interface depends on its effective mass and friction (Colour figure online)

where G(0) is the free energy at zero field. Thus the difference between the two phases is

$$\Delta G_{AB}(B) = \Delta G_{AB}(0) - \frac{1}{2}\chi_{AB}B^2 \tag{2}$$

where χ_{AB} is the difference in susceptibilities between the A and B phases. At the transition field the Gibbs free energy difference is zero, $\Delta G_{AB}(B_c) = 0$. Hence $\Delta G_{AB}(0) = \frac{1}{2}\chi_{AB}B_c^2$, giving

$$\Delta G_{AB}(B) = \frac{1}{2}\chi_{AB}\left(B_c^2 - B^2\right). \tag{3}$$

Suppose that the interface is at a vertical position z_I and that it moves in a uniform vertical field gradient ∇B. The field at the interface is $B = B_c + \nabla B(z_I - z_{eq})$ so the corresponding force on the interface is

$$F(z) = -A\chi_{AB}B_c|\nabla B|\left(z_I - z_{eq}\right). \tag{4}$$

where $A = \pi D^2/4$ is the cross-sectional area of the sapphire tube. Equation (4) gives the restoring force directed towards the equilibrium position with a spring constant per unit area

$$k = \chi_{AB}B_c|\nabla B|. \tag{5}$$

In general the interface will also experience inertial and frictional forces, so the equation of motion of a planar interface can be written as

$$m\ddot{z}_I + \gamma\dot{z}_I + k(z_I - z_{eq}) = 0, \tag{6}$$

where m is the effective mass per unit area of the interface and the friction coefficient γ is the dissipative force per unit area per unit velocity. In the following we suppose that m and γ are constant during the interface motion.

The interface is driven by applying a small uniform oscillating field $B_{ac}e^{i\omega t}$ which produces an oscillation in the equilibrium position

$$z_{eq} = \frac{B_{ac}}{|\nabla B|}e^{i\omega t}. \tag{7}$$

The resulting oscillation of the interface can be written as $z_I = z_0 e^{i\omega t}$. Substituting z_I and z_{eq} in Eq. (6), and then solving for the amplitude gives

$$z_0 = \frac{k}{k - m\omega^2 + i\omega\gamma}\left(\frac{B_{ac}}{|\nabla B|}\right). \tag{8}$$

The ensuing power dissipated by the moving interface is $\dot{Q}_{diss} = A\gamma\dot{z}_I^2$. Substituting for $\dot{z}_I$ using Eq. (8) and taking the time average gives the average power dissipation

$$\langle\dot{Q}_{diss}\rangle = \frac{A}{2}\gamma\frac{k^2\omega^2}{(k - m\omega^2)^2 + (\gamma\omega)^2}\left(\frac{B_{ac}}{|\nabla B|}\right)^2. \tag{9}$$

In the low frequency limit the interface moves with the equilibrium position z_{eq}, the amplitude of motion is $B_{ac}/|\nabla B|$, and the average dissipation is

$$\langle \dot{Q}_{diss} \rangle_{\omega \to 0} = \frac{A}{2} \gamma \omega^2 \left(\frac{B_{ac}}{|\nabla B|} \right)^2. \tag{10}$$

In the high frequency limit the interface lags behind the equilibrium position and the dissipation becomes independent of the field gradient

$$\langle \dot{Q}_{diss} \rangle_{\omega \to \infty} = \frac{A\gamma}{2} \frac{\chi_{AB}^2 B_c^2 B_{ac}^2}{m^2 \omega^2 + \gamma^2}. \tag{11}$$

Experimental results for the measured average dissipation from an oscillating interface are shown in Fig. 3 for three different field gradients, reproduced from our earlier report [19]. The measurements were made at temperatures around $155\,\mu K$ and at 0 bar pressure, using the techniques discussed in Sect. 2. The data at low frequencies, below $\approx 2\,Hz$, fit quite well to Eq. (9) with $m = 0$ and a constant value for γ [19]. Setting the effective mass term to zero was consistent with the theoretical expectation of a negligibly small effective mass arising from differences in the densities of the A phase, B phase and planar-like phase across the interface [1,18]. However, the inferred value for γ was orders of magnitude greater than the theoretical estimates of Leggett and Yip, and of Kopnin, for Andreev scattering and for pair-breaking [1,18,20]. Further, the increase in dissipation for frequencies above 2 Hz could not be explained by existing theories.
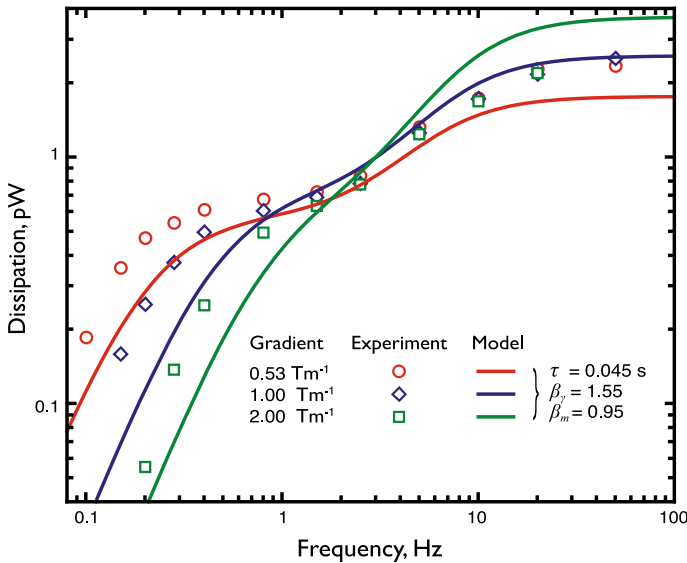

Fig. 3 The dissipation of the oscillating A–B boundary versus frequency. The points show measurements at a field oscillation amplitude of $B_{ac} = 0.64\,mT$ for three different field gradients. The lines are fits to the model, see text (Colour figure online)

4 Friction and Effective Mass Due to the Orbital Texture

We first consider the A phase, whose order parameter is highly anisotropic for all values of the magnetic field. The energy gap has nodes along the orbital axis l_A [22]. The preferred orientation of l_A is perpendicular to the magnetic field, perpendicular to the cell walls, and parallel to the plane of the A–B interface. In the experimental geometry illustrated in Figs. 1 and 2, all of these preferences can be accounted for by having a texture where l_A lies in the horizontal plane, albeit with at least one textural defect. For this configuration motion of the interface does not require any change in the orientation of l_A so the orbital texture does not couple to the interface dynamics. This may not be the case close to the cell walls where the A-phase meniscus bends upwards to make a contact angle [9] of approximately 70°. This occurs over a relatively small length scale so we neglect its effect on the interface dynamics.

Conversely, in the B phase the orbital texture across the whole cross-section of the cell is affected by the A–B interface and its motion. In a magnetic field, the energy of a quasiparticle excitation with momentum p and spin $\sigma\hbar$ is given by [27,28]

$$E_{p,\sigma} = \sqrt{(E_\parallel(\mathbf{p}) - \sigma\hbar\widetilde{\omega}_L)^2 + (\Delta_\perp p_\perp)^2} \tag{12}$$

where $E_\parallel(\mathbf{p}) = (\xi^2 + \Delta_\parallel^2 p_\parallel^2)^{\frac{1}{2}}$ and $\xi = (p - p_F)v_F$ is the kinetic energy relative to the Fermi energy. Here $\Delta_\parallel$ and $\Delta_\perp$ are the energy gaps parallel and perpendicular to l_B, $p_\parallel$ and $p_\perp$ are the parallel and perpendicular components of the quasiparticle momentum, p_F is the Fermi momentum and v_F is the Fermi velocity. The Fermi-liquid corrected quasiparticle Zeeman energy is $\sigma\hbar\widetilde{\omega}_L$ with $\sigma = \pm 1/2$. In practice, the Zeeman splitting dominates the anisotropy and so $\Delta_\parallel$ and $\Delta_\perp$ can be approximated by the zero field gap Δ_0 [28–30].

The minimum quasiparticle energy as a function of the angle between its momentum and the l_B axis is shown in Fig. 4a. At temperatures far below T_c the vast majority of excitations occupy the lowest energy states with momenta centred around the l_B axis. Motion of the interface changes the local orientation of l_B in the vicinity of the interface which thus changes the quasiparticle energies as illustrated in the figure. The subsequent relaxation of the excitations occurs over a time scale τ. This is the essential mechanism for providing the effective mass and friction of the interface. Below we develop a preliminary model to describe how this affects the interface dynamics.

For a cylindrical tube parallel to a magnetic field, the preferred orientation of l_B is given by the "flare-out" texture [31–33]. This texture has l_B oriented parallel to the field direction along the tube axis, and bending radially so that it is perpendicular to the sidewalls. The healing length ξ_B over which l_B changes direction is inversely proportional to the magnitude of the field [31–34], and for fields close to B_c we estimate $\xi_B \approx 0.1\,\text{mm}$ [5,32,34,35]. This is much smaller than the tube radius in our experiments so as a first approximation we may neglect the influence of the walls and assume that the B-phase l_B texture far from the interface is uniform and parallel to the vertical field.

However, close to the interface it is energetically favourable for l_B to be oriented parallel to the interface [5]. Thus in our experimental configuration far away from
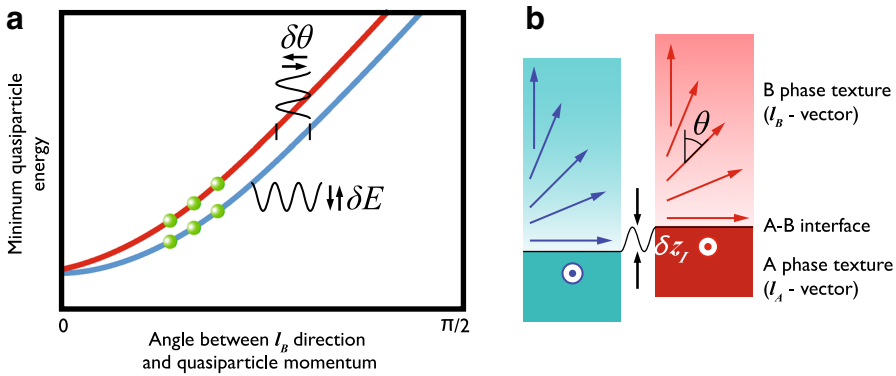
Fig. 4 Schematic of the effects of orbital motion in the B-phase texture induced by an oscillating A–B interface. **a** The minimum energy of a quasiparticle excitation in the B-phase texture. Oscillation of the texture induces oscillations in the quasiparticle energies. **b** As the A–B interface moves the A-phase texture is unchanged, and our simple model assumes that the whole B-phase texture moves with the interface, see text. The subsequent change in the quasiparticle energies results in an effective mass of the interface and dissipation (friction) (Colour figure online)

the interface the l_B texture is vertical, but approaching the interface it must rotate to become horizontal. The change in orientation occurs over a distance of order ξ_B from the interface. This texture is illustrated in Fig. 4b where θ denotes the angle between l_B and the vertical.

A change in the orientation of l_B by an amount $\delta\theta$ changes the quasiparticle energies by

$$\delta E_{p,\sigma} = \frac{\partial E_{p,\sigma}}{\partial \theta} \delta\theta \tag{13}$$

which produces a viscous torque [36,37]

$$\boldsymbol{\Gamma}_{vis} = -\mu \boldsymbol{l}_B \times \dot{\boldsymbol{l}}_B = -\mu \dot{\boldsymbol{\theta}}, \tag{14}$$

where μ is the orbital viscosity. We find the corresponding force on the interface by considering the work done by the viscous torque and equating it to the work done by the moving interface.

To simplify the problem we suppose that the orbital texture in the B phase responds instantaneously to the changing position of the interface. This means that we neglect the orbital dynamics and suppose that l_B always has its equilibrium orientation $\theta(z - z_I)$ relative to the position of the interface, as illustrated in Fig. 4b. This simplification is ultimately justified here by the model capturing the essential behaviour of the experimental data; a fuller treatment in future ought to take into account the dynamics of the l_B texture itself.

Consider a small change in position of the interface δz_I. This causes the texture orientation in the B phase to adjust by

$$\delta\theta(z) = \frac{\partial \theta}{\partial z_I} \delta z_I \tag{15}$$

and thus

$$\dot{\theta} = \frac{\partial \theta}{\partial z_I} \dot{z}_I. \tag{16}$$

The corresponding work done on the quasiparticle distribution is

$$\delta W = \int_V \Gamma_{vis} \delta\theta dV \tag{17}$$

where $\Gamma_{vis} = |\mathbf{\Gamma}_{vis}| = \mu\dot{\theta}$ and the integral is over the whole volume of the B phase. Substituting for Γ_{vis} and using Eqs. (15) and (16) we find

$$\delta W = \int_V \mu\left(\frac{\partial \theta}{\partial z_I}\right)^2 \dot{z}_I \delta z_I dV. \tag{18}$$

The force exerted by the moving interface has reactive and dissipative components corresponding to the inertial and frictional force respectively $F = A(m_l\ddot{z}_I + \gamma_l\dot{z}_I)$, where the subscript denotes the contributions from the viscous torque due to the changing $\mathbf{l}_B$ texture. For oscillatory motion $\ddot{z}_I = i\omega\dot{z}_I$ so the work done on moving the interface by δz_I can be written as

$$\delta W = A(\gamma_l + i\omega m_l)\dot{z}_I \delta z_I. \tag{19}$$

Equating this with the work done on the quasiparticles, Eq. (18), and substituting $dV = Adz$ gives

$$\gamma_l + i\omega m_l = \mu \int_z \left(\frac{\partial \theta}{\partial z_I}\right)^2 dz. \tag{20}$$

Thus the friction coefficient γ_l is related to the real part of the orbital viscosity and the effective mass of the interface m_l is related to the imaginary part.

The orbital viscosity in the B phase at low temperatures was previously shown to be [21]:

$$\mu = \frac{\tau + i\omega\tau^2}{1 + (\omega\tau)^2}\left[\frac{\pi}{6}N(0)\frac{\Delta}{k_B T}\exp\left(-\Delta/k_B T\right)(\hbar\widetilde{\omega}_L)^2\right] \tag{21}$$

to first order in $\widetilde{\omega}_L^2$, where τ is quasiparticle collision time, $N(0)$ is the normal density of states at the Fermi surface, and Δ is approximately equal to the zero field gap Δ_0.

We can estimate the integral in Eq. (20) by supposing that θ decays exponentially from $\frac{\pi}{2}$ to zero over the textural healing length ξ_B,

$$\theta(z) = \frac{\pi}{2}\exp\left(-(z - z_I)/\xi_B\right). \tag{22}$$

The integral in Eq. (20) is then evaluated as

$$\int_z \left(\frac{\partial \theta}{\partial z_I} \right)^2 dz = \frac{\pi^2}{8\xi_B}. \tag{23}$$

Substituting Eqs. (21) and (23) in Eq. (20) gives the following estimates for the friction coefficient

$$\gamma_l = \frac{\tau}{1 + (\omega\tau)^2} \left[\frac{\pi}{6} N(0) \frac{\Delta}{k_B T} \exp\left(-\Delta/k_B T\right) (\hbar\widetilde{\omega}_L)^2 \right] \frac{\pi^2}{8\xi_B} \tag{24}$$

and the effective mass

$$m_l = \frac{\tau^2}{1 + (\omega\tau)^2} \left[\frac{\pi}{6} N(0) \frac{\Delta}{k_B T} \exp\left(-\Delta/k_B T\right) (\hbar\widetilde{\omega}_L)^2 \right] \frac{\pi^2}{8\xi_B}. \tag{25}$$

To evaluate γ_l and m_l for the experimental data in Fig. 3 we use the following values: $\hbar\widetilde{\omega}_L = 0.67\Delta_0$, from [28–30]; $\Delta_0 = 1.76 k_B T_c$ with $T_c = 0.929$ mK at 0 bar pressure, from [38]; $N(0) = 1.0 \times 10^{51}$ m^{-3}, from [38,39]; $\xi_B = 0.1$ mm, from [5,32,34,35]; and $T = 155 \, \mu$K (noting that this is an average temperature, and the actual temperature during the measurements varied from $T = 150 \, \mu$K to $T = 160 \, \mu$K as the dissipation increased from low to high frequencies). The value of quasiparticle relaxation τ is the only unknown parameter.

To compare the model predictions with the experimental data in Fig. 3 we introduce two additional fitting parameters β_γ and β_m for the magnitudes of the friction coefficient and effective mass respectively

$$\gamma = \beta_\gamma \gamma_l \tag{26}$$

$$m = \beta_m m_l \tag{27}$$

The fits shown in Fig. 3 were made with $\beta_\gamma = 1.55$, $\beta_m = 0.95$ and $\tau = 0.045$ s. For clarity, we have used the same fitting parameters for all three sets of data. Better fits can be obtained by changing the parameters for each set of data, but given the simplicity of the model we do not believe that this reveals any significant new information.

5 Discussion

The values of the fitting parameters β_γ and β_m are both close to unity. This suggests that orbital motion in the B phase is the dominant mechanism for determining both the friction coefficient and the effective mass of the A–B interface. The friction coefficient γ determines the low frequency response of the interface, below a few Hz for the data shown in Fig. 3. At the lowest frequencies, the interface moves with the equilibrium position and the dissipation is given by Eq. (10). At slightly higher frequencies the dissipation reaches a plateau as the interface lags behind the equilibrium position. The quasiparticle relaxation time determines the second rise in dissipation at a frequency

$f \approx 1/(2\pi\tau)$. This rise only occurs when the interface is over-damped, with $\beta_\gamma > \beta_m$. In the under-damped case, a dissipation peak occurs at a frequency $f \approx \sqrt{k/m}/(2\pi)$. It will be interesting to investigate whether such a peak can be observed experimentally. The effective mass parameter β_m determines the location of the second plateau at the highest frequencies.

The fitted value for the quasiparticle relaxation time $\tau = 0.045$ s is of order a hundred times larger than the transit time of a quasiparticle moving between the walls of the cell, $\tau_{wall} \approx D/v_g$, where the mean quasiparticle group velocity v_g is roughly one third of the Fermi velocity for our experimental conditions. This is the expected order of magnitude since the vast majority of excitations have insufficient energy to propagate through the changing texture close to the wall. These excitations are Andreev reflected and effectively form bound states within the texture. Only a small fraction of excitations, $\sim 1\%$, are able to scatter with the cell wall and contribute to the quasiparticle relaxation.

To conclude, we have shown that orbital motion in the high field distorted B phase of superfluid ^{3}He can account for the dissipation and the effective mass of an oscillating A–B interface at low temperatures. Our simple model gives a reasonable fit to the experimental data. A more sophisticated model will need to take into account the precise dynamics of the orbital texture, the effects of cell walls and the role of Andreev scattering within the texture.

References

1. A.J. Leggett, S.K. Yip, in *Helium 3*, ed. by W.P. Halperin, L.P. Pitaevskii (North Holland, Amsterdam, 1990)
2. M.C. Cross, in *Quantum Fluids and Solids*, ed. by S.B. Trickey, et al. (Plenum Press, New York, 1977)
3. R. Kaul, H. Kleinert, J. Low Temp. Phys. **38**, 539 (1980)
4. N. Schopohl, Phys. Rev. Lett. **58**, 1664 (1987)
5. E.V. Thuneberg, Phys. Rev. B **44**, 9685 (1991)
6. M. Bartkowiak, S.W.J. Daley, S.N. Fisher, A.M. Guénault, G.N. Plenderleith, R.P. Haley, G.R. Pickett, P. Skyba, Phys. Rev. Lett. **83**(17), 3462 (1999)
7. M. Bartkowiak, S.N. Fisher, A.M. Guénault, R.P. Haley, G.N. Plenderleith, G.R. Pickett, P. Skyba, Physica B **280**(1–4), 108 (2000)
8. D.D. Osheroff, M.C. Cross, Phys. Rev. Lett. **38**, 905 (1977)
9. M. Bartkowiak, S.N. Fisher, A.M. Guénault, R.P. Haley, G.R. Pickett, M.C. Rogge, P. Skyba, J. Low Temp. Phys. **126**(1–2), 533 (2002)
10. M. Bartkowiak, R.P. Haley, S.N. Fisher, A.M. Guénault, G.R. Pickett, P. Skyba, Physica B **329**, 122 (2003)
11. M. Bartkowiak, D.I. Bradley, S.N. Fisher, A.M. Guénault, R.P. Haley, G.R. Pickett, P. Skyba, J. Low Temp. Phys. **134**(1–2), 387 (2004)
12. M. Bartkowiak, S.N. Fisher, A.M. Guénault, R.P. Haley, G.R. Pickett, P. Skyba, Phys. Rev. Lett. **93**(4), 045301 (2004)
13. G. Volovik, *The Universe in a Helium Droplet* (Oxford University Press, Oxford, 2003)

14. C. Bäuerle, Y.M. Bunkov, S.N. Fisher, H. Godfrin, G.R. Pickett, Nature **382**, 332 (1996)
15. V.M.H. Ruutu, V.B. Eltsov, A.J. Gill, T.W.B. Kibble, M. Krusius, Y.G. Makhlin, B. Plaçais, G.E. Volovik, W. Xu, Nature **382**, 334 (1996)
16. D.I. Bradley, S.N. Fisher, A.M. Guénault, R.P. Haley, J. Kopu, H. Martin, G.R. Pickett, J.E. Roberts, V. Tsepelin, Nat. Phys. **4**(1), 46 (2008)
17. D. Buchanan, G. Swift, J. Wheatley, Phys. Rev. Lett. **57**(3), 341 (1986)
18. A.J. Leggett, S. Yip, Phys. Rev. Lett. **57**, 345 (1986)
19. M. Bartkowiak, S.N. Fisher, A.M. Guénault, R.P. Haley, G.N. Plenderleith, G.R. Pickett, P. Skyba, Physica B **284**, 240 (2000)
20. N.B. Kopnin, Sov. Phys. JETP **65**, 1187 (1987)
21. S. Fisher, N. Suramlishvili, J. Low Temp. Phys. **138**(3–4), 771 (2005)
22. D. Vollhardt, P. Wölfle, *The Superfluid Phases of Helium 3* (Taylor & Francis, London, 1990)
23. S.N. Fisher, A.M. Guénault, C.J. Kennedy, G.R. Pickett, Phys. Rev. Lett. **69**, 1073 (1992)
24. S.N. Fisher, A.M. Guénault, C.J. Kennedy, G.R. Pickett, Phys. Rev. Lett. **63**, 2566 (1989)
25. C. Bäuerle, Y.M. Bunkov, S.N. Fisher, H. Godfrin, Phys. Rev. B **57**, 14381 (1998)
26. I. Hahn, Y.H. Tang, H.M. Bozler, C.M. Gould, Physica B **194**(1), 815 (1994)
27. N. Schopohl, J. Low Temp. Phys. **49**(3–4), 347 (1982)
28. M. Ashida, K. Nagai, Prog. Theor. Phys **74**, 949 (1985)
29. K. Nagai, Private Communication
30. S.N. Fisher, PhD Thesis, Lancaster, 1991
31. H. Smith, W.F. Brinkman, S. Engelsberg, Phys. Rev. B **15**(1), 199 (1977)
32. P.J. Hakonen, M. Krusius, M.M. Salomaa, R.H. Salmelin, J.T. Simola, A.D. Gongadze, G.E. Vachnadze, G.A. Kharadze, J. Low Temp. Phys. **76**, 225 (1989)
33. W.F. Brinkman, H. Smith, D.D. Osheroff, E.I. Blount, Phys. Rev. Lett. **33**(11), 624 (1974)
34. O. Ishikawa, Y. Sasaki, T. Mizusaki, A. Hirai, M. Tsubota, J. Low Temp. Phys. **75**, 35 (1989)
35. J. Kopu, Private Communication
36. M.C. Cross, J. Low Temp. Phys. **26**(1–2), 165 (1977)
37. W.F. Brinkman, M.C. Cross, in *Progress in Low Temperature Physics*, ed. by D.F. Brewer (Elsevier, Oxford, 1978)
38. D.S. Greywall, Phys. Rev. B **33**, 7520 (1986)
39. J.C. Wheatley, Rev. Mod. Phys. **47**, 415 (1975)